Available online at www.sciencedirect.com
SCIENCE DIRECT®
Acta Materialia 53 (2005) 1931–1944
Acta MATERIALIA
www.actamat-journals.com

Mechanical behavior of Σ tilt grain boundaries in nanoscale Cu and Al: A quasicontinuum study

F. Sansoz [a,*], J.F. Molinari [b]

[a] Department of Mechanical Engineering, The University of Vermont, 201B Votey bldg, 33 Colchester Avenue, Burlington, VT 05405, USA
[b] Department of Mechanical Engineering, Johns Hopkins University, 3400 North Charles Street, Baltimore, MD 21218, USA

Received 23 September 2004; received in revised form 8 December 2004; accepted 6 January 2005
Available online 1 February 2005

Abstract

Molecular simulations using the quasicontinuum method are performed to understand the mechanical response at the nanoscale of grain boundaries (GBs) under simple shear. The energetics and mechanical strength of 18 Σ ⟨1 1 0⟩ symmetric tilt GBs and two Σ ⟨1 1 0⟩ asymmetric tilt GBs are investigated in Cu and Al. Special emphasis is placed on the evolution of far-field shear stresses under applied strain and related deformation mechanisms at zero temperature. The deformation of the boundaries is found to operate by three modes depending on the GB equilibrium configuration: GB sliding by uncorrelated atomic shuffling, nucleation of partial dislocations from the interface to the grains, and GB migration. This investigation shows that (1) the GB energy alone cannot be used as a relevant parameter to predict the sliding of nanoscale high-angle boundaries when no thermally activated mechanisms are involved; (2) the E structural unit present in the period of Σ tilt GBs is found to be responsible for the onset of sliding by atomic shuffling; (3) GB sliding strength in the athermal limit shows slight variations between the different interface configurations, but has no apparent correlation with the GB structure; (4) the metal potential plays a determinant role in the relaxation of stress after sliding, but does not influence the GB sliding strength; here it is suggested that the metal potential has a stronger impact on crystal slip than on the intrinsic interface behavior. These findings provide additional insights on the role of GB structure in the deformation processes of nanocrystalline metals.

Keywords: Grain boundary structure; Grain boundary cohesion; Nanocrystalline materials; Simulation; Quasicontinuum method

1. Introduction

The influence of grain boundary (GB) structure on the mechanical behavior of bicrystals and polycrystals has been the subject of intense interest for many decades because interfaces exert profound effects on deformation mechanisms [1,2]. In recent years, considerable research efforts [3–8] have been focused on the mechanical behavior of fully dense nanocrystalline metals, which contain nanosized grains (<100 nm), and thus a substantial volume fraction of GBs and triple junctions. The above studies are motivated by the fact that for nanocrystalline metals, deformation mechanisms strongly differ from those found in their coarse-grained counterparts, and result in unique, superior mechanical characteristics. Molecular simulations and experiments have revealed that deformation mechanisms in nanocrystalline metals at room temperature are influenced by four parameters: grain size [6–9], the metal tested [7,8], magnitude of the applied stress [7,10], and structure of the GB network [11,12]. As grain size increases from a few nanometers to several tens of nanometers, a transition exits from GB-mediated deformation processes involving GB sliding or GB migration [6–9,13–16], to intragranular lattice

* Corresponding author. Tel.: +1 802 656 3837; fax: +1 802 656 1929.
E-mail address: frederic.sansoz@uvm.edu (F. Sansoz).

1359-6454/$30.00 © 2005 Acta Materialia Inc. Published by Elsevier Ltd. All rights reserved.
doi:10.1016/j.actamat.2005.01.007

activities involving full dislocations [7,8,10], extended partial dislocations [6–8,16] and mechanical twins [17–21]. While the origin of intragranular processes in nanocrystalline metals is under intense debate at present time, two factors having strong impact on the intragranular regime have been identified, namely the generalized planar fault energy curve [8], which varies based on the metal interatomic potential, and the driving force necessary to trigger intragranular mechanisms, which may be hindered locally in the presence of structural relaxations at the GB [7,8].

For smaller grain size (<15 nm), stress-induced GB sliding may operate in nanocrystalline metals at room temperature [6–9,13,15,16]. This result is in contrast with well-established results on microscale polycrystals, where GB sliding is dominated by thermally activated mechanisms [1]. In nanocrystalline metals, GB sliding results from individual atom shuffling events, i.e., a process in which a GB atom transfers directly from one grain to another without the creation of point defects [1,22]. Even at low temperature, this unique process is shown to cause cooperative grain rotations without the presence of permanent crystal lattice deformation [9,23–26]. It is acknowledged that the structure of GB network plays an important role in cooperative GB activities. For example, it is considered that general high-angle GBs are lesser obstacles to sliding than low-energy twin boundaries [25]; see recent works of Lu and co-workers [27] showing drastic changes in the mechanical behavior of nanocrystalline metals when nano-twin boundaries are grown instead of randomly oriented GBs.

Despite the common knowledge that GB structure does influence intergranular and intragranular modes of deformation in nanocrystalline metals, the incidence of GB structure on the mechanical response of a GB is not fully understood at the nanoscale, particularly in the athermal regime. This task is made complicated by the fact that the constitutive response of a grain boundary, which is usually obtained by testing a bicrystal, accounts for both interface behavior (atom shuffling, sliding, GB dislocations and defects) and grain bulk behavior (lattice dislocations) as reviewed in the next section. Furthermore, only the relevant information obtained from atomic scale processes at the boundaries should be taken into account in order to address the challenge of scales involved in the hierarchical modeling of deformation of nanocrystalline materials. No consensus, however, exists as to the relation between interface deformation and GB structure parameters in nanocrystalline materials. In the present study, we carried out a series of molecular simulation on nanosized bicrystals under shear in order to shed light onto fundamental deformation mechanisms taking place in nanocrystalline GBs, when no thermally activated GB mechanisms operate. Our intent was twofold: (i) to gain understanding of the constitutive response of a GB at the nanoscale, and (ii) to identify a structure parameter relevant to nanomechanical response. The paper is divided as follows. Section 2 is intended to review the literature relative to the mechanical properties of GBs and to emphasize the recent advances in this field using atomistic models. Section 3 presents the details of the computational procedure based on the quasicontinuum method, used here to simulate the simple shear at zero temperature of nanosized bicrystals containing a GB. In Section 4, we report on the results of simulations performed on 18 $\langle 1\,1\,0\rangle$ symmetric tilt GBs and 2 $\langle 1\,1\,0\rangle$ asymmetric tilt GBs using the interatomic potential for Cu and Al. In Section 5, we show the existence of a structural unit in the GB period responsible for the onset of GB sliding by atomic shuffling. In light of this result, we discuss in this section the effects of GB structure and metal potential on the mechanical response at the nanoscale of GBs under simple shear.

2. Review on the mechanical response of crystalline interfaces at nanoscale

2.1. GB structure and energetics

The works of Kumar et al. [24], Stern et al. [28], and Van Swygenhoven et al. [29] provide support for the hypothesis that GB structure in nanocrystalline metals does not strongly differ from that found in coarse-grained metals. In the above studies, it has been found that nanocrystalline metals have a large degree of order, and are made of structural units, which are usually observed in conventional high-angle GBs. For low-angle boundaries, GB dislocation networks have also been observed in nanocrystalline metals regardless of the grain size [29]. These results preclude nanocrystalline interfaces being highly disordered, amorphous-like boundaries. Therefore, conclusions drawn in the present study on the basis of nanoscale bicrystals with well-controlled GB structures are to some extent representative of generic nanocrystalline interfaces. Strong correlations are known to prevail between structure and energy in GBs [30–33]. In particular, Wolf [34] has demonstrated using molecular dynamics calculations that the correlation between energy and volume expansion of relaxed GBs does not significantly change if the GB character is symmetric, asymmetric, tilt, twist, special or random. This result suggests that the GB energy may be related to a structure parameter independent of tilt angle, tilt axis, metal potential, and GB plane orientation. Earlier atomistic studies have been focused on symmetric tilt GB structures, where high-angle boundaries can be described using simple structural units [35], and low-angle boundaries with GB dislocation networks. However, the overview given by Randle [36] on the generic GB structure of Cu and Ni boundaries with $\langle 1\,1\,0\rangle$ tilt and $\Sigma 3^n$

systems shows that those actual boundaries are asymmetric. In contrast, Singh and King [37] have equally observed symmetric and asymmetric in deposited, textured thin Au films. These observations coupled with the lack of statistical data currently available on the GB networks of nanocrystalline materials, suggest that a better understanding of GB deformation must be gained on both symmetric and asymmetric tilt GBs.

2.2. Implications of atomic structure on GB deformation

The mechanical response of nanoscale GBs under shear has been described by Farkas [38] as follows. Most rigid-body translations around a stable configuration do not result in a new GB structure but merely induce a distortion of the existing structure and build-up elastic stresses in the surrounding crystal lattice. According to Farkas, a transition to a different structure occurs when the local shear stress at the boundary reaches a critical level, necessary to induce GB sliding. Farkas' analysis suggests considering three constitutive parameters in the shear response of GBs: (1) the modulus of rigidity corresponding to the elastic bulk behavior; (2) the maximum level of stress before sliding; and (3) the level of stress after sliding.

It has been shown that the sliding resistance of GBs depends on both boundary atomic interactions and GB structure. Dorfman et al. [39,40] for instance have compared the shear behavior of $\Sigma3(1\,1\,1)$ twins in tungsten using pairwise or many-body interactions potentials. These authors have concluded that the number of energy peaks associated with the γ-surfaces for this GB is smaller with pairwise potentials. By means of rigidly deforming bicrystals using 2D molecular dynamics, Chandra and co-workers [41,42] have also proposed considering a direct correlation between GB energy and GB sliding distance in Al symmetric tilt boundaries; here the lower the GB energy, the smaller the sliding distance. This conclusion is supported by a large number of studies on thermally activated GB sliding, showing that faster GB sliding occurs due to higher GB self-diffusion rates, which correlates with both GB energy and GB volume [1].

Furthermore, Hoagland and Kurtz [43] and de Koning et al. [44] have reported that the transmission of lattice dislocations across $\Sigma11$ tilt GBs in Al does significantly change depending on the degree of symmetry of the interface, because the distribution and magnitude of local energy peaks become highly heterogeneous in asymmetric GBs. The above results imply that local energy variations, which are caused by localized structure changes in the interface, must also be considered in addition to the average GB energy. The works of Molteni et al. [45], Suzuki and Mishin [46,47], Kurtz et al. [48,49], and Derlet et al. [50] on nanocrystalline metals are in line with this hypothesis. The above authors have found that the deformation mechanisms are strongly related to the migration of local, point defects in the interface. Derlet et al. [50] have investigated in nanocrystals the role of point defects and dislocations present in the GB regions on the mechanism of partial dislocation nucleation. Their work has shown that the emission of partial dislocations from GBs is the consequence of local atom shuffling events and stress-assisted free volume migration in the boundaries. As a consequence, the deformation of nanocrystalline interfaces has been found to operate by four fundamental mechanisms: interface migration [45,51], GB sliding accompanied by atom shuffling [46,47], GB-mediated dislocation emission [50], and/or nanocrack formation at triple junctions [24,52,53].

Finally, it is worth emphasizing the contribution of athermal effects in the GB sliding behavior of nanocrystalline materials. Schiotz and co-workers have simulated the deformation of nanocrystalline copper in the intergranular regime at both zero temperature [15] and finite temperature [54]. These authors have shown using molecular dynamics that GB sliding remains the main deformation mechanism at all grain sizes up to 13 nm, even at zero temperature. It may be assumed in general that the strength of GB against sliding is a superposition of athermal and thermally activated effects. However, the results of Schiotz and co-workers show that interfaces in nanocrystalline metals, where a diffusional explanation is not relevant at zero temperature, may indeed be dominated by the athermal contribution to GB sliding. While the influence of GB structure on the thermally activated sliding behavior has been well-documented, it is unclear how GB structure influences the GB sliding mechanism in the athermal limit. The results of zero temperature simulations are presented here in order to shed light on this specific aspect.

2.3. Size effects on the mechanical response of crystalline interfaces

The mechanical response of crystalline interfaces at the nanoscale, and particularly the maximum boundary strength, is strongly dependent upon the size of the computational cell under applied loading. This is due to the fact that boundary constraints play an important role on the deformation mechanisms triggered from the interface. In an earlier investigation, the present authors have examined the influence of boundary constraints on the mechanical behavior of a copper $\Sigma9(2\,2\,1)$ symmetric tilt GB under tension and shear [55]. Atomistic simulations have been performed on cells containing a bicrystal in which several crystal lattice planes parallel to, and near the interface were kept unconstrained, while the reminder of the cell had a constrained, homogeneous displacement. The major results of this investigation are reported in Fig. 1.

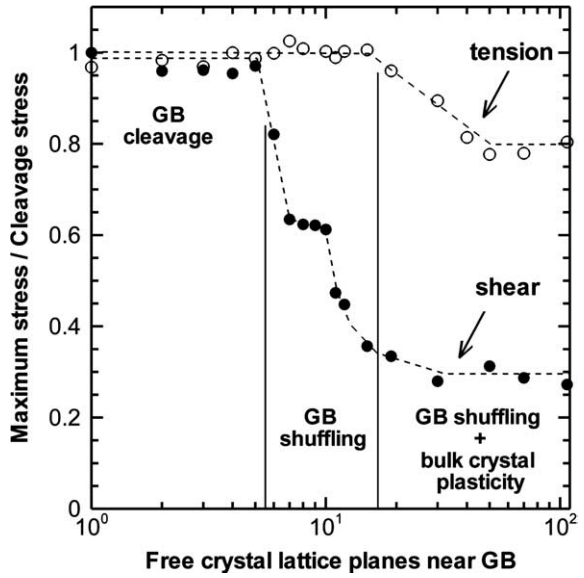

Fig. 1. Size effects on the maximum strength and deformation mechanisms of a Σ9(221) symmetric ⟨110⟩ tilt GB in Cu under tension or shear loading. Results reported in Ref. [55].

Under shear displacement, it has been observed that the maximum boundary strength decreases up to 70% as the number of free crystal lattice planes near the GB is increased. The loss of boundary strength in this case was accompanied by a change of deformation mechanism from quasi-cleavage fracture to GB atom shuffling process and, subsequently, to atom shuffling plus bulk crystal plasticity in the form of partial dislocations emitted from the GB. In contrast, under tension, GB atom shuffling processes were absent; here the deformation mechanism varied directly from cleavage to bulk crystal plasticity, and the loss of boundary strength was only of 20%. This indicates that GB-mediated plasticity, i.e., in this context, GB atom shuffling, causes a strong decrease of the maximum GB strength. In addition, it has been shown that, in this GB-mediated regime, the maximum shear stress was constant regardless of the size of the model, while crystal lattice plasticity was absent. The following conclusions can be drawn from the above investigation: (1) the mechanical behavior of a bicrystal containing a GB at its center combines interface behavior and crystal lattice plasticity; nanoscale crystal plasticity is GB-mediated by non-local deformation gradients emerging from interface processes; (2) atomic-scale shuffling in the GB region strongly impacts on the maximum GB strength; and (3) size effects on the mechanical response of nanoscale GBs are significant under shear loading only.

3. Computational technique

A cell containing a bicrystal with a GB at its center is simulated using the quasicontinuum method developed by Tadmor and co-workers [56–58]. The quasicontinuum method is a molecular static technique finding the solution of equilibrium atomic configurations by energy minimization, given externally imposed forces or displacements. The problem is modeled without explicitly representing every atom in the cell; here regions of small deformation gradients are treated as a continuum media by the finite element method. For example, the quasicontinuum mesh for a Σ27(552) ⟨110⟩ symmetric tilt bicrystal in Cu is shown in Fig. 2. It is worth emphasizing that in this scheme the connection between continuum and full atomistic is made in a seamless manner, i.e., that there is no discontinuity in the energy state at the continuum/atomistic frontier. A detailed overview of the quasicontinuum implementation is given in Ref. [58]. The constitutive law in continuum and atomistic domains is an embedded-atom-method (EAM) potential. The EAM potential provided by Foiles et al. [59] for Cu and that from Ercolessi and Adams [60] for Al are used here. These potentials lead to cutoff distances of 4.950 and 5.558 Å, respectively. The atoms in the GB region are all represented within a distance from the GB plane equal to 7.5 times the potential cutoff distance. A typical simulation is performed with less than 8000 nodes.

Each bicrystal is constructed using the coincident site lattice (CSL) model and the Bravais lattice cell [61] as follows. The simulation cell is considered quasi-planar with only one repeated CSL cell along the tilt vector, **c**, contained in the GB plane. This constraint is imposed by the current implementation of the quasicontinuum method. The investigated tilt axis is along the $[1\underline{1}0]$ direction. The tilt angle of the upper and lower grains, referred to as ψ and ψ' in the following, is defined by the angle between the [110] crystal direction and the normal **n** of the GB plane; see Fig. 3(a). Two types of tilt GB structure are studied: symmetric GBs ($\psi = \psi'$) and asymmetric GBs ($\psi \neq \psi'$). The CSL cell is repeated periodically along the **n** and $\mathbf{n} \otimes \mathbf{c}$ axes such that the size of each grain is kept between 50 and 70 Å along the **n** direction, and a mesh aspect ratio is maintained close to 4. The latter condition is used in order to avoid discrepancies in the force/energy calculations because of free surface effects [62]. The minimum dimensions for the entire bicrystal at equilibrium are about 400 Å × 100 Å × 5 Å. The simulation cell is relaxed under zero force lattice static at zero temperature in order to obtain the lowest state of energy for a given GB configuration. In this process, all atoms in line at the bottom of the lower grain are constrained, thereby avoiding crystal rotation. The energy minimization process is performed using a conjugate gradient method. The total energy is minimized until the addition of out-of-balance forces over the entire system is found less than 10^{-3} eV/Å. Before relaxation, a spacing of 3 Å is introduced in the **n** direction between the grains allowing for GB volume expansion and trans-

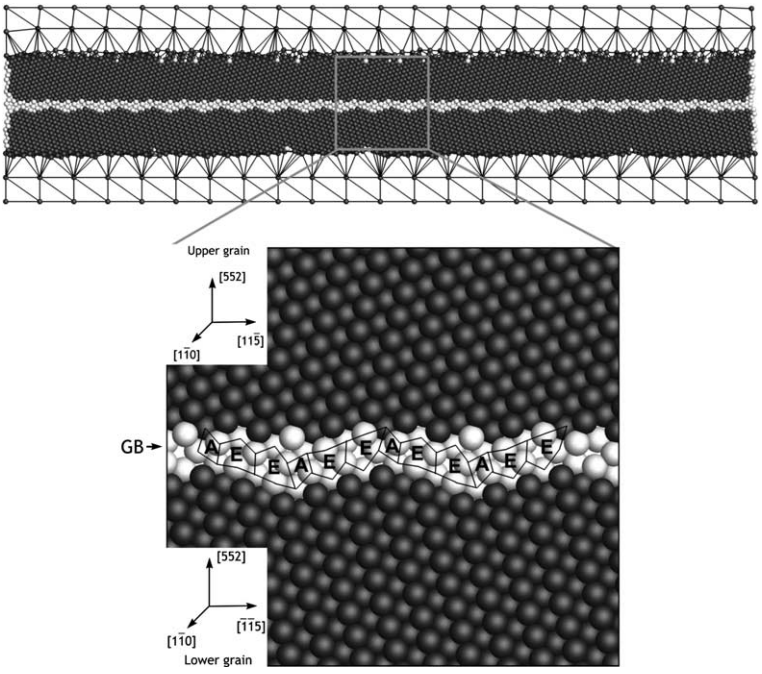

Fig. 2. Quasicontinuum model of a Σ27(5 5 2) symmetric tilt grain boundary in copper. Dark-colored atoms are in perfect fcc crystal lattice (centrosymmetry parameter = 0). Bright-colored atoms are in the vicinity of crystal defects, stacking faults and free surfaces (centrosymmetry parameter > 0.25). The crystals orientation and grain boundary position after relaxation are indicated. Two periods of boundary structural units (A:E:E:A:E:E) are also represented in the grain boundary region.

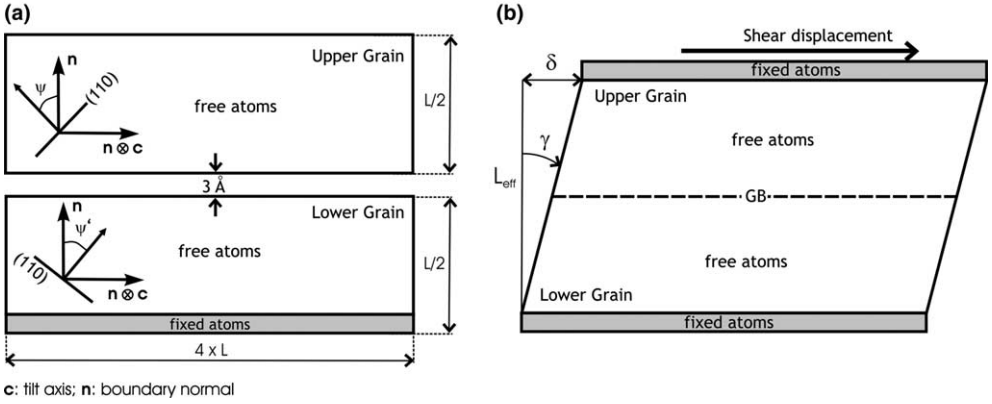

Fig. 3. Boundary conditions of (a) zero force lattice statics for 0 K equilibrium GB structure and (b) simple shear loading.

verse shifting of the upper grain relative to the lower grain during energy minimization. Because the initial grain shifting may also cause to reach a metastable GB structures, several initial configurations are tested, provided that one of the initial configurations leads to the lowest state in energy after atomic relaxation. The initial shift vector in these configurations is defined by the displacement-shift-complete lattice [61]. Only the results obtained for GBs with the lowest state of energy are reported in the following. In addition, it is shown below that the equilibrium structures obtained by this technique are in excellent agreement with those found using conventional molecular dynamics on symmetric tilt GBs [35] and asymmetric tilt GBs [38,44] in face-centered cubic (fcc) metals. Simple homogeneous shear is performed by straining the relaxed bicrystal in a series of incremental shear displacement on the top line of atoms in the upper grain along the $\mathbf{n} \otimes \mathbf{c}$ direction, which is parallel to the GB plane as shown in Fig. 3(b). The atoms on the right and left sides of the cell are free of constraints. Between each load step, the strain increment is kept less than 0.15%, and a new energy minimization is performed. The bottom line of atoms in the lower grain is kept fixed in all directions. The top line of atoms in the upper grain is fixed in the **n** direction. The latter boundary condition was found

to have negligible impact on the calculated shear stress, while maintaining a certain degree of homogeneity in the deformation patterns over the entire GB length. The displacement of all atoms in the simulation cell is constrained along the tilt direction, **c**. The shear strain γ is given by:

$$\gamma = \arctan\left(\frac{\delta}{L_{\text{eff}}}\right).$$

In this expression, δ is the imposed shear displacement. L_{eff} is the size of the unconstrained atomic region. The GB energy is calculated by subtracting the bulk single crystal energy to the bicrystal energy and dividing by the GB area. To limit surface effects in the energy calculation, only 80% of the bicrystal is considered, therefore excluding atoms near free surfaces.

Details on the calculation of stress and analysis of deformation processes are described in this section. The definition of virial stress [63] agrees with the continuum definition of stress in the case of uniform strains in a bulk crystal. It has been recognized, however, that the virial definition can be significantly different from the continuum stress near free surfaces [64]. In light of this fact, the present authors have exercised caution in making any direct comparisons between the atomic-level and continuum definitions of stress, because the current problem contains significant free surfaces. In the present study, the shear stress is calculated by adding the residual forces at the top of the upper grain and dividing by the GB area. Similar to the calculations of GB energy, only 80% of the bicrystal is considered in the stress calculation; see above. The current procedure can be interpreted as an estimate of the average "far-field" stress without the need for the calculation of local stress variations across the boundary. Despite the approximation made in the stress definition, the authors have shown in earlier works [55] that the calculated stress is in excellent agreement with the average stress obtained on molecular dynamics studies of single crystal. Interestingly, this agreement holds even with GB structures; see for comparison the results obtained by Spearot et al. [65] using molecular dynamics simulations. In order to detect planar defects and GB structure with respect to the elastically deformed crystal domain, the centrosymmetry parameter P proposed by Kelchner et al. [66] is used in accordance with the following definition:

$$P = \sum_{i=1,6} |R_i + R_{i+6}|^2,$$

where R_i and R_{i+6} are the vectors or bonds corresponding to the six pairs of opposite nearest neighbors in a 3D fcc lattice. We modified this expression in the case of a quasi-2D lattice by calculating the centrosymmetry parameter on three pairs of closest neighbors projected in the tilt plane. In practice, we find that a threshold of $P = 0.25$ allows for the detection of a stacking fault left behind partial dislocations in Cu and Al. For other type of defects, i.e., point defects, full dislocation, and free surface atoms, the centrosymmetry parameter is found to be greater than 0.25. The atoms are colored according to the value of the centrosymmetry, appearing in dark color with perfect fcc stacking ($P < 0.25$) and in bright color with crystal defects ($P > 0.25$).

4. Results

4.1. Atomic structure and energy of grain boundaries at equilibrium

Nine $\langle 1\,1\,0\rangle$ symmetric tilt GB configurations corresponding to different misorientation angles ($\psi = \psi'$) were created in both Cu and Al. The GB energy and structural unit period calculated from those configura-

Table 1
Constitutive parameters of copper tilt grain boundaries under shear

Type	(hkl) GB plane	$\psi + \psi'$ (°)	Energy (mJ/m^2)	Structural unit period	Mechanical behavior		
					$\sigma_{\max}$ (GPa)	σ_{d} (GPa)	Deformation mode
STGB	Σ27(5 5 2)	31.58	870	|AEEAEE|	2.07	1.23	GB shuffling and partial nucleation
	Σ33(4 4 1)	20.04	863	|AAEAAE|	1.90	0.87	GB shuffling only
	Σ9(2 2 1)	38.94	833	|EE|	1.39	0.62	GB shuffling and partial nucleation
	Σ11(3 3 2)	50.48	699	|DEDE|	1.68	0.96	GB shuffling and partial nucleation
	Σ27(1 1 5)	148.4	699	|CBA|[a]	2.96	0.96	GB migration
	Σ73(6 6 1)	13.44	674	|A′A′E′A′A′|[a]	1.03	0.85	GB migration
	Σ33(5 5 4)	59.00	488	|DDDE″DDDE″|	1.61	1.14	Dissociated stacking faults from GB
	Σ11(1 1 3)	129.52	309	|CC|[a]	5.41	2.56	Partial nucleation from GB
	Σ3(1 1 1)	70.52	9	|D|[a]	2.35	1.22	Twin migration
ATGB	Σ11(2 2 5)/(4 4 1)	39.52	680	|CDCDA′|	3.08	2.73	Dissociated stacking faults from GB
	Σ121(1 1 0)/(7 7 1 2)	39.52	701	|DA′DACDDD… …EDDDACEDD|	1.55	1.29	GB shuffling only

STGB, symmetric tilt grain boundary; ATGB, asymmetric tilt grain boundary.
[a] Structural unit period with mirror symmetry across the interface.

Table 2
Constitutive parameters of aluminum symmetric tilt grain boundaries (STGB) under shear

Type	(*hkl*) GB plane	$\psi + \psi'$ (°)	Energy (mJ/m^2)	Structural unit period	Mechanical behavior		
					σ_{max} (GPa)	σ_d (GPa)	Deformation mode
STGB	Σ27(552)	31.58	490	|AEEAEE|	1.17	1.01	GB shuffling only
	Σ9(221)	38.94	483	|CB|[a]	0.63	0.42	GB migration
	Σ33(441)	20.04	427	|E′E′A|[a]	1.99	1.64	GB migration
	Σ11(332)	50.48	407	|DEDE|	1.66	0.81	GB shuffling and twin emission
	Σ27(115)	148.4	389	|BB|[a]	3.50	1.89	Partial nucleation from GB
	Σ73(661)	13.44	376	|A′A′E′A′A′|	2.39	2.21	Point defects migration
	Σ33(554)	59.00	290	|DDDE″DDDE″|	1.19	1.18	Dissociated stacking faults
	Σ11(113)	129.52	131	|CC|[a]	3.11	2.59	Partial nucleation from GB
	Σ3(111)	70.52	59	|D|[a]	1.05	0.76	Twin migration

[a] Structural unit period with mirror symmetry across the interface.

tions at 0 K equilibrium are given in Tables 1 and 2 for Cu and Al, respectively. The coincident site parameter Σ corresponds to the reciprocal density of coincident sites at the interface of two grains. The Σ value of the high-angle GBs studied here ranges from 3 to 33, while the unique boundary with low misorientation angle (13.4°) has a Σ value of 73. The GB energies are represented in Fig. 4 as a function of the tilt angle. It is shown in this figure that the calculated energies are in excellent agreement with the reference energies determined in earlier studies using quasi-planar molecular dynamics [32,41]. It is important to note that the GB energy strongly varies with respect to the misorientation angle, i.e., cusps in the energy state associated with the ⟨110⟩ tilt axis exist for the Σ3(111) coherent twin and Σ11(113) boundary at a tilt angle of 70.52° and 59.00°, respectively. Fig. 4 also reveals that for the same grain misorientation, the corresponding GB energy is almost twofold larger in Cu than in Al. The GB energies vary from 9 to 870 mJ/m^2 for Cu and from 59 to 490 mJ/m^2 for Al. With fcc Σ tilt GBs, each interface promotes a structural period made of a small number of individual structural units. In the current investigation, we found seven compact structural units in the interfaces, which were also reported by Rittner and Seidman [35] in Ni, and Suzuki and Mishin [47] in Cu and Al. Those structural units are illustrated in Fig. 5 on the period of four investigated GBs. While two structural units (A and C) are made of four atoms placed in diamond, the B structural unit connects nine atoms by a hexagonal prism. The D structural unit is a simple stacking fault line linking two atoms. A structural unit playing a key role on mechanical behavior, as shown in the next sections, is the E structural unit composed of six atoms interconnected by a capped trigonal prism. The E′ structural unit is a rotated and elongated E structural unit which has a mirror symmetry across the interface. Similarly, the A′ structural unit is an A structural unit rotated by 90°. Additionally, we found in Cu and Al a structural unit, referred to as E″ in the following, which is the combination of the E structural unit with an intrinsic stacking fault extending over few atomic planes in the crystal; see Fig. 5(d). As shown in Tables 1 and 2, the E structural units were often found in the period of high-energy GBs such as Σ27(552) or Σ9(221). This is due to the delocalized, asymmetric character of this structural unit as well as to the large volume expansion needed to accommodate this unit. GBs with mirror symmetry

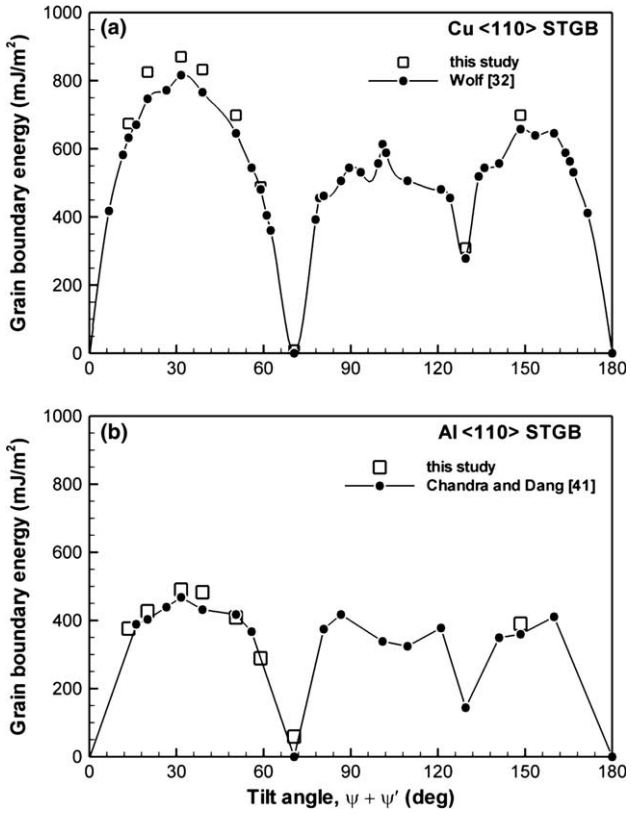

Fig. 4. Grain boundary energies of the 0 K equilibrium structure for ⟨110⟩ symmetric tilt grain boundaries investigated in (a) copper and (b) aluminum, as a function of tilt angle between grains. Calculated energies are compared to reference energies obtained on quasi-planar embedded-atom-method molecular dynamics simulations.

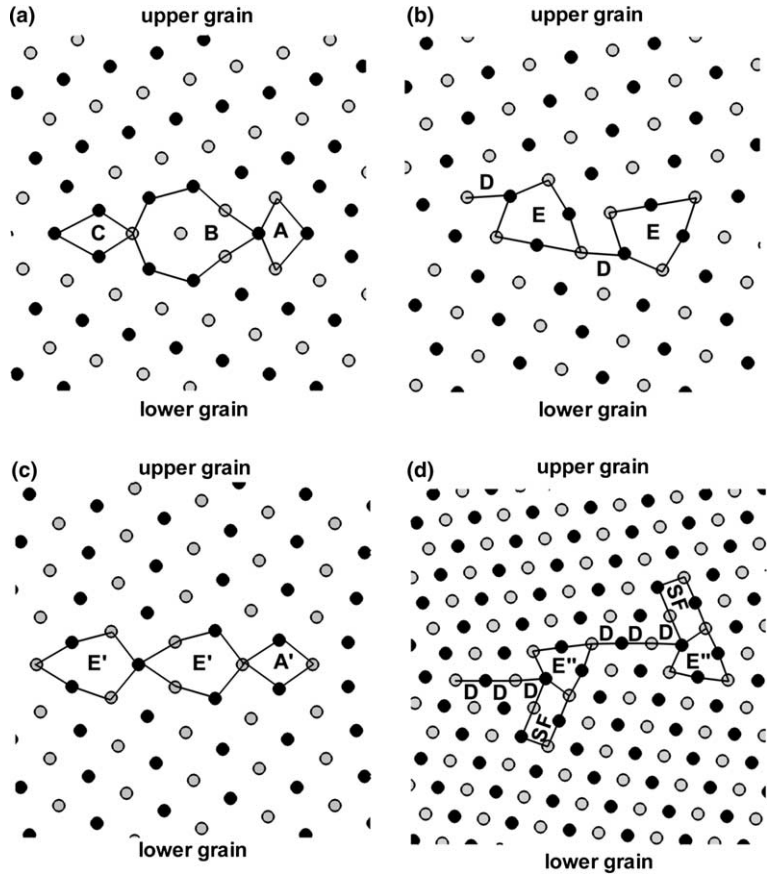

Fig. 5. Illustration of eight individual structural units (A,A′,B,C,D,E,E′,E″) composing the period of $\Sigma\langle 1\,1\,0\rangle$ symmetric tilt GBs in fcc metals at 0 K equilibrium: (a) $\Sigma 27(1\,1\,5)$ GB in Cu; (b) $\Sigma 11(3\,3\,2)$ GB in Cu; (c) $\Sigma 33(4\,4\,1)$ GB in Al; and (d) $\Sigma 33(5\,5\,4)$ GB in Cu. Dark and open circles are atoms on two different $(1\,\bar{1}\,0)$ planes.

across the interface are marked by an asterisk in those tables. The latter type of boundary was preferentially found in Al or with low-energy boundaries in Cu. For the same GB configuration and tilt misorientation, it is worth noting that the structural unit period tends to change between Cu and Al when the GB energy becomes relatively high with the notable exception of the $\Sigma 27(5\,5\,2)$ symmetric GB. For instance, it is shown in Table 1 that the $\Sigma 9(2\,2\,1)$ symmetric GB in Cu exhibit the period |EE| without mirror symmetry across the interface, while in Table 2 the same boundary is found having a period |CB| with mirror symmetry. It will be shown below that the change of GB structure with respect to the metal potential has a profound impact on the deformation mode of the GB.

The structure of $\Sigma 11(2\,2\,5)/(4\,4\,1)$ and $\Sigma 121(1\,1\,0)/(7\,7\,1\,2)\ \langle 1\,1\,0\rangle$ asymmetric GBs was also investigated in Cu; see Fig. 6. These GBs were also studied by de Koning et al. [44] in Al and by Farkas [38] in nanocrystalline Ni, respectively. The energy of the $\Sigma 11(2\,2\,5)/(4\,4\,1)$ GB was found to be equal to 680 mJ/m^2 in Cu, while that of the $\Sigma 121(1\,1\,0)/(7\,7\,1\,2)$ GB is 701 mJ/m^2. It is noteworthy that the energy calculated on these non-special, asymmetric boundaries is slightly smaller than the maximum GB energy found on special, symmetric boundaries. This provides some support to the idea that the energy of special GBs is not fundamentally different from that in random nanocrystalline interfaces. The structural unit period of the $\Sigma 11(2\,2\,5)/(4\,4\,1)$ GB involves A′, C, and D structural units. The period of the $\Sigma 121(1\,1\,0)/(7\,7\,1\,2)$ GB is more complex, and involves a combination of A, A′, C, D, and E structural units. Our results show the dissociation at equilibrium of the asymmetric GBs into stacking faults emanating from the GB (Shockley partials), while the GB structures reported in the literature in Al and Ni did not present this effect. This discrepancy can be interpreted by the fact that different interatomic potentials have been used for Al and Ni, which were associated with higher stacking fault energies than for the Cu potential used in the present study.

4.2. Mechanical response for different GB structures

This section focuses on the evolution of the average stress for different bicrystals as a function of the ap-

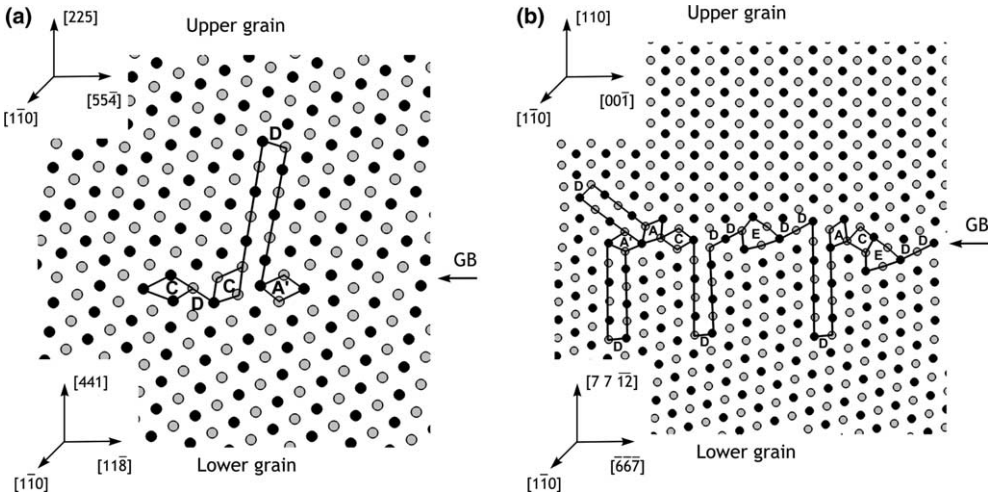

Fig. 6. Structural unit period of ⟨1 1 0⟩ asymmetric tilt GBs investigated in Cu: (a) Σ11(2 2 5)/(4 4 1) GB; and (b) Σ121(1 1 0)/(7 7 12) GB.

plied shear strain. Fig. 7 shows the mechanical response of four GBs under shear at zero temperature. This figure reveals two trends which can be described as follows. As shear strains are applied, each bicrystal initially deforms elastically; here stress and strain are proportional with a modulus of rigidity, G. Subsequently, the simulation cell reaches a maximum level of stress σ_{max}, occurring in Fig. 7(a) for a shear strain γ of about 4%, after which the curve drops abruptly from σ_{max} to the value σ_d, more so for Cu than Al. In the trend shown in Fig. 7(a), the stress relaxation is associated with the sliding of the GB. This is followed for increased shear strains by a less smooth stress profile; however, the stress curve tends to form a plateau. This behavior, which is found for instance in the shear of the high-energy Σ27(5 5 2) symmetric GB, is somewhat reminiscent of a stick–slip process. The trend shown in Fig. 7(b) is different from the above response because the first stress relaxation is followed by a new elastic loading step associated with the same modulus of rigidity. When σ_{max} is reached a second time, the stress drops again, and the process repeats itself as above. This type of behavior was found associated with the migration of the GB in the direction perpendicular to the interface, and as a consequence, this constitutive response is referred to as migration-type in the following. In both stick–slip and migration-type responses, the modulus of rigidity has limited variations with respect to the GB structure. The modulus of rigidity was found equal to

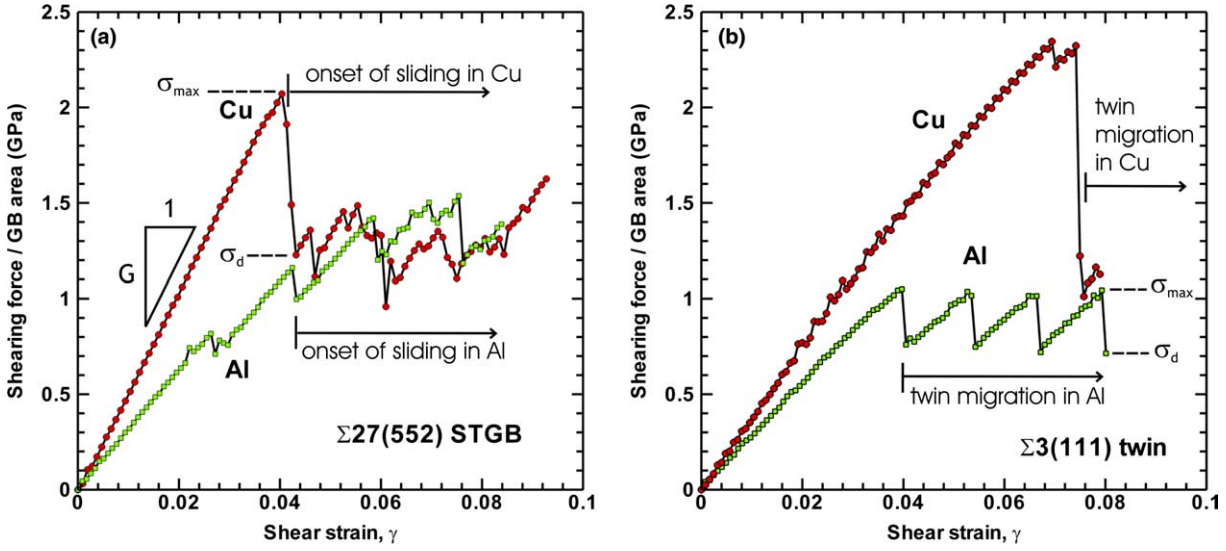

Fig. 7. Mechanical response under shear of: (a) Σ27(5 5 2) symmetric tilt grain boundary; and (b) Σ3(1 1 1) twin boundary in copper and aluminum. The onset of boundary sliding or boundary migration starts where indicated.

48.6 ± 8.5 GPa in Cu and 29.7 ± 3.4 GPa in Al. The critical stress values σ_{max} and σ_d are given for each GB in Tables 1 and 2. Those values are found to change significantly based on the GB configuration. Qualitatively, it can be observed that σ_{max} has a higher value in Cu than Al except for the Σ33(5 5 4) symmetric GB. The latter may be due to the presence of stacking faults which extend further away from the interface in Cu than in Al.

4.3. Analysis of deformation mechanisms in relation to the mechanical response

The simulation performed on the GB structures examined above led to three predominant modes of deformation, which have also been reported in the literature on nanocrystalline metals. The deformation mechanisms are summarized for each boundary in Tables 1 and 2. Associated with the mechanical response shown

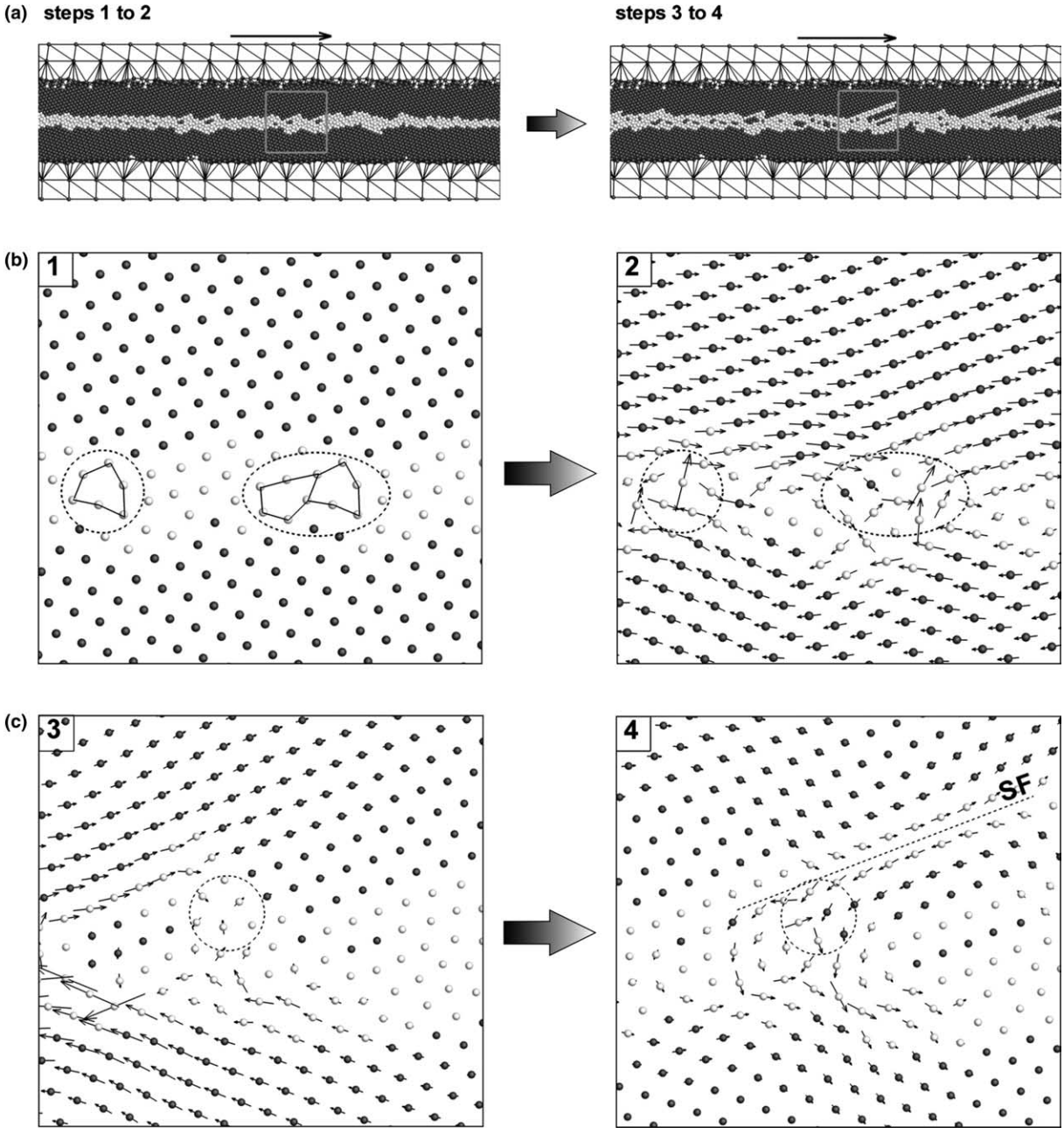

Fig. 8. (a) Zero temperature deformation modes of a Σ27(5 5 2) ⟨1 1 0⟩ symmetric tilt GB in Cu; uncorrelated atom shuffling of the interface occurring from after reaching the maximum applied stress (load steps 1 and 2); partial dislocation emission from the GB occurring subsequently (steps 3 to 4). (b) Enlarged region of GB atom shuffling processes with arrows indicating the incremental displacement from load steps 1 to 2, and circles emphasizing the site of E structural units. (c) Enlarged region of partial dislocation emission from GB.

in Fig. 7(a), we observed that the stress relaxation accompanying GB sliding results from atomic shuffling events localized in the boundary. This is shown in Figs. 8(a) and (b) with the deformation of a Σ27(5 5 2) symmetric tilt GB in Cu. Arrows in Fig. 8(b) indicate the direction and magnitude of the displacement for each boundary atom between two load steps taken before and after reaching σ_{max}. It is shown in step 2 of this figure that the behavior of a few GB atoms is uncorrelated with the reminder of the bicrystal, where atoms are homogeneously shifted parallel to the interface. It should be emphasized that the centrosymmetry is not changed in the grains during atom shuffling, indicating that this process of deformation is localized at the interface. For clarity, we circled the regions of atomic shuffling. The figure also shows that atom shuffling events are initiated from E structural units. During this process, we observed that a free volume left by one of the E structural units, moves within the boundary, as the strain increases. In the second stage of deformation of the Σ27(5 5 2) symmetric GB corresponding to strains exceeding 4%, the free volume regions travel by additional shuffling. Fig. 8(c) shows that a free volume which is circled is the site for the nucleation and propagation of a partial dislocation. The emitted partial dislocation is seen in step 4 of this figure with the bright-colored atoms pointing out a stacking fault left behind the dislocation in the upper crystal. It is important to note that in some GB configurations such as the Σ27(1 1 5) symmetric GB or Σ11(1 1 3) symmetric GB in Al, atom shuffling is absent, and the bicrystal deforms only by the nucleation of partial dislocations from the interface. In those cases, the maximum GB strength against shear was found to be significantly high.

The second mode of GB motion related to the curves shown in Fig. 7(b) corresponds to the collective atom migration of the interface perpendicular to the loading direction; see Fig. 9. In this process, the interface migrates discontinuously as the shear is applied, i.e., the bicrystal deforms elastically up to the level of stress σ_{max}, subsequently leading to sudden GB migrations. The deformation mode of the Σ33(5 5 4) symmetric GBs in Al and Cu is an exception to the above mechanisms. The Σ33(5 5 4) symmetric GBs, which were initially dissociated into extended stacking faults after equilibrium, were found to deform by the propagation of the dissociated faults in the crystal, and neither shuffling nor migration processes occur in this case.

Tables 1 and 2 reveal a strong correlation between the occurrence of GB sliding by atom shuffling, and the presence of E structural units in the GB period regardless of tilt orientation, symmetry or metal potential. This aspect will be discussed in the next section. It also appears clearly that the maximum shear strength σ_{max} of GBs sliding by atomic shuffling has slight variations, but no correlation with respect to the initial GB configuration. To put this result into perspective, the maximum shear stress for different sliding boundaries was represented in Fig. 10 as a function of the GB energy E. The latter was normalized by the product of the modulus of rigidity and the crystal lattice $G \times a$ as suggested in Ref. [47] when comparing different metal potentials. In this figure, the average value of maximum shear strength is found equal 1.63 GPa with small variations of ±0.46 GPa. However, no general trends between maximum shear strength and structure were found for GBs which do not slide, but deform by migration or the nucleation of partial dislocations only. Finally, the magnitude of the stress relaxation $|\sigma_{max} - \sigma_d|$ appears higher in Cu than in Al regardless of the GB structure. The average relaxation was found equal to 0.96 GPa in Cu, and 0.46 GPa in Al.

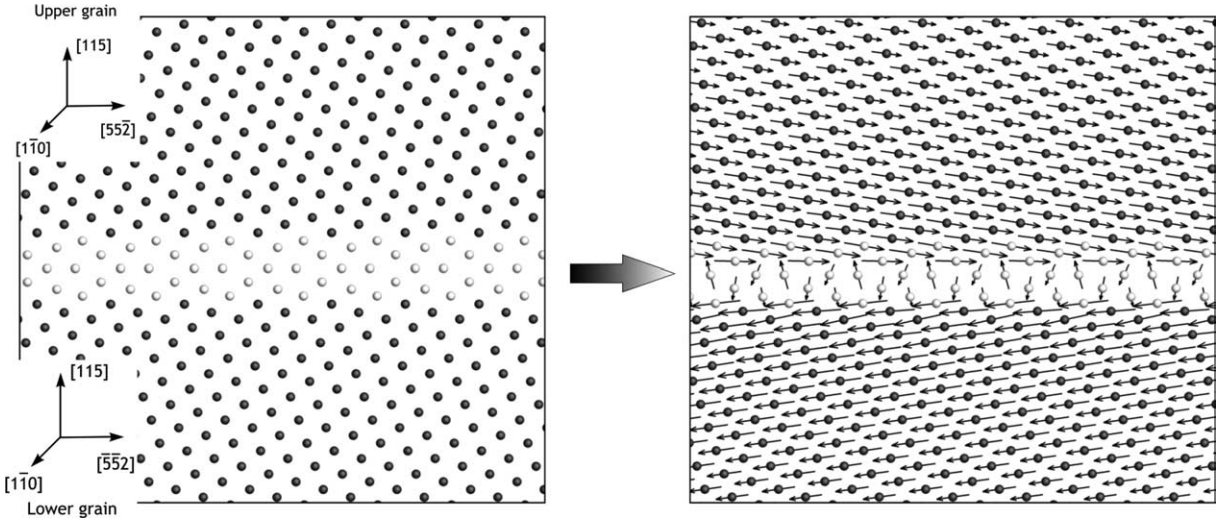

Fig. 9. Deformation of a Σ27(1 1 5) symmetric tilt grain boundary in copper resulting in collective atom migration at maximum applied stress.

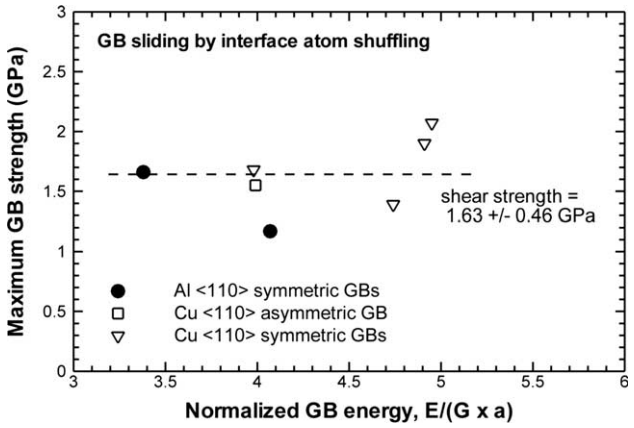

Fig. 10. Maximum shear strength of $\Sigma\langle 1\,1\,0\rangle$ tilt bicrystals sliding by atom shuffling at the interface as a function of the normalized GB energy, $E/(G\times a)$.

5. Discussion

5.1. Structural unit conditioning GB sliding

GB sliding processes in the athermal limit were found to operate at nanoscale by atomic shuffling events localized at the interface, which is in line with reports in the literature on the deformation of nanocrystalline metals. One of the main findings in this study is that a direct correlation exists between the onset of GB sliding and the presence of E structural units in the GB period. The boundaries containing E structural units tend to be high-energy boundaries because this unit causes pronounced GB expansion to accommodate large free volumes. The present study also demonstrates that the GB energy alone cannot be used to determine the propensity for a GB to slide at zero temperature, which differs from the usual explanation established by previous atomistic studies [41,42] involving thermal effects. An obvious example is given in the following for Al. The $\Sigma27(5\,5\,2)$ symmetric GB, which has the highest state of energy at equilibrium (490 mJ/m^2), and the $\Sigma11(3\,3\,2)$ symmetric GB are the only Al boundaries deforming by GB sliding. The $\Sigma11(3\,3\,2)$ symmetric GB, however, has a smaller state of energy at equilibrium (407 mJ/m^2) than the $\Sigma9(2\,2\,1)$ symmetric GB (487 mJ/m^2) or $\Sigma33(4\,4\,1)$ symmetric GB (427 mJ/m^2). The latter boundaries do not present any E structural units and deform by GB migration in Al, implying that the structural unit rather than the GB energy is a pertinent parameter here.

An evidence of structural relevance is also found with four of the GBs in Cu having close GB energies: the $\Sigma11(3\,3\,2)$ symmetric GB (699 mJ/m^2), the $\Sigma27(1\,1\,5)$ symmetric GB (699 mJ/m^2), the $\Sigma121(1\,1\,0)/(7\,7\,1\,2)$ asymmetric GB (701 mJ/m^2), and the $\Sigma11(2\,2\,5)/(4\,4\,1)$ asymmetric GB (680 mJ/m^2). Both $\Sigma11(3\,3\,2)$ symmetric GB and $\Sigma121(1\,1\,0)/(7\,7\,1\,2)$ asymmetric GB promote GB sliding by atom shuffling, as opposed to the $\Sigma27(1\,1\,5)$ symmetric GB and $\Sigma11(2\,2\,5)/(4\,4\,1)$ asymmetric GB, which deform by GB migration and propagation of dissociated stacking faults, respectively. It is important to note that the structural unit period of the former GBs is made of two E structural units from which the onset of atom shuffling was observed. It should also be noticed that the presence of dissociated stacking faults seen after equilibrium of certain interfaces, which often form E″ structural units from the core of E structural units, seems to prevent atom shuffling; here the dissociated stacking faults simply propagate in the grains when a shear strain is applied. It is noteworthy that GBs made of E″ structural units such as the $\Sigma33(5\,5\,4)$ symmetric GB have relatively small energies (488 mJ/m^2 in Cu and 290 mJ/m^2 in Al).

In summary, the onset of GB sliding at the nanoscale is found to occur in Σ tilt GBs whenever the GB structure is associated to relatively high GB energies and E structural units. At zero temperature, while a high GB energy seems necessary for triggering GB sliding, it is not a sufficient parameter.

5.2. Resistance against GB sliding in the athermal limit

At the nanoscale, the simple shear behavior of a sliding GB is reminiscent of a stick–slip process. This emphasizes the necessity to allow for the stress relaxation of the boundary in the determination of GB mechanical properties using atomistic simulations. As shear strains increase, elastic strains build up until a maximum stress is reached; thereby leading to a new GB configuration. This new configuration is obtained by atomic shuffling of the interface through the mechanism described above. The maximum shear stress reached before GB sliding is referred to as GB sliding strength in the following. An important conclusion of this investigation is that the GB sliding strength varies slightly at 0 K, but with no direct correlation with respect to the GB structure at equilibrium. Its average value was found to be equal to 1.63 GPa with small variations in stress of ± 0.46 GPa. This result can be interpreted by considering the E structural unit as vacancies located in the boundary. In their work on the diffusion of points defects in fcc GBs, Suzuki and Mishin [46,47] have shown that the energy for vacancy migration becomes high if the vacancy is moved toward the crystal bulk; thereby, vacancy migration remains short-range, and always confined within a few layers near the boundary. Therefore, the stress-induced migration behavior of vacancies in GBs, as suggested by Suzuki and Mishin, should not be considered influenced by the delocalization of the vacancies, regardless of the initial GB configuration.

We have also observed no direct correlation of the number of E structural units on the GB sliding strength. This result suggests that a local analysis of the stress distribution along the interface would be a better way to interpret the change in mechanical strength between different GB configurations. This is in line with the fact that, in our model without diffusional assumption, the structure of GBs has a more complex influence on GB sliding than if thermal effects were considered. It would be worth analyzing the GB-mediated behavior of nanostructured metals on the same basis, since athermal effects may also become significant on the interface sliding of this class of materials [15,54].

It can be pointed out once more that not all GB structures lead to sliding, for which case the mechanisms of GB migration or nucleation of partial dislocations from the GB are favored. A second important observation is that the behavior of GBs deforming by the latter modes is more significantly influenced by the crystal bulk rather than by the GB structure itself. In the current study, this assumption is supported by the fact that no relation between GB structure and strength could be directly established for those modes of deformation.

5.3. Effects of metal potential on GB deformation

The effects of metal potential are evident on the GB energy at equilibrium as well as on the stress relaxation after reaching σ_{max}. For the same initial configuration, the GB energy is found to be twofold less in Al than in Cu at equilibrium. One possible explanation is the tendency of high-energy GBs to relax differently in Cu and Al, thereby leading to different GB structures at equilibrium. This result may also be correlated to the difference in the planar stacking fault energy between the two metals. On the other hand, the differences in stress relaxation may rather be associated, as suggested by Van Swygenhoven et al. [8] for nanocrystalline slip, by the difference in the ratio between the unstable stacking fault energy and the planar stacking fault energy of the grains. This is in accordance with the fact that the $\Sigma 11(3\,3\,2)$ symmetric GB was found to nucleate only partial dislocations in Cu, but also mechanical twins in Al at the same level of stress, 1.68 and 1.66 GPa, respectively. Furthermore, the $\Sigma 11(1\,1\,3)$ symmetric GBs deform by emitting partial dislocations without atomic shuffling in both Al and Cu. In this example, the first partial dislocation is emitted at a stress value of 5.41 and 3.11 GPa in Cu and Al, respectively, but the stress relaxes to the same level of 2.6 GPa in both materials. It may be envisaged on this basis that it is easier in Al to nucleate a trailing partial, which will subsequently cause mechanical twinning, than in Cu because the stress relaxation is less significant in Al. This observation provides additional insights to explain the differences obtained in the onset of crystal slip in nanocrystalline metals, with respect to the metal potential used.

6. Conclusions

A series of quasicontinuum simulations have been performed to understand the mechanical response at zero temperature of a GB at the nanoscale in Cu and Al. Twenty $\langle 1\,1\,0\rangle$ tilt GB configurations have been tested under simple shear. The principal conclusions of this investigation can be drawn as follows.

The modes of deformation of Σ tilt GBs in Cu and Al were found to operate by GB sliding caused by the atomic shuffling of the interface, collective GB migration, or nucleation of stacking faults and dislocations from the interface to the grains. Our major observation is that the onset of GB sliding is directly linked to the presence of E structural units in the GB period. In the athermal limit, while a high GB energy seems necessary for triggering GB sliding, it is demonstrated that the GB energy is not a sufficient parameter. Additionally, the GB sliding strength corresponding to the maximum shear stress before atomic shuffling is found to vary slightly, but with no direct correlation with respect to the equilibrium GB structure or metal potential.

These results provide additional insights to design nanostructured metals made of nano-sized grains, and supplement our understanding of GB sliding when no thermally activated mechanisms operate. It is acknowledged that, for small grain sizes (<15 nm), intragranular plastic deformation is almost absent, and the strength and ductility of nanostructured metals is GB-mediated. The results of this investigation suggest that improved ductility can be achieved by forming GBs containing particular structural units which favor the onset GB sliding by atomic shuffling. However, it is not clear at present how the observed variations in GB sliding strength impact the overall strength of nanostructured metals.

Acknowledgments

This work was performed under the auspices of NSF-Nanoscale Interdisciplinary Research Team under contract DMR-0210215 and ARL-Center for Advanced Materials and Ceramic Systems under the ARMAC-RTP Cooperative Agreement Number DAAD 19-01-2-0003. F.S. acknowledges support from NSF-Vermont Experimental Program to Stimulate Competitive Research (VT EPSCoR) under Grant number NSF EPS 0236976. We are also grateful to R. Miller and E. Tadmor for providing the quasicontinuum code [67].

References

[1] Sutton AP, Balluffi RW. Interfaces in crystalline materials. Oxford: Clarendon Press; 1995.
[2] Balluffi RW, Sutton AP. Mater Sci Forum 1996;207–209:1.
[3] Weertman JR, Farkas D, Hemker K, Kung H, Mayo M, Mitra R, et al. MRS Bull 1999(February):44.
[4] Robertson A, Erb U, Palumbo G. Nanostruct Mater 1999;12:1035.
[5] Kumar KS, Van Swygenhoven H, Suresh S. Acta Mater 2003;51:5743.
[6] Schiotz J, Jacobsen KW. Science 2003;301:1357.
[7] Yamakov V, Wolf D, Phillpot SR, Mukherjee AK, Gleiter H. Nat Mater 2004;3:43.
[8] Van Swygenhoven H, Derlet PM, Froseth AG. Nat Mater 2004;3:399.
[9] Lund AC, Nieh TG, Schuh CA. Phys Rev B 2004;69:012101.
[10] Yamakov V, Wolf D, Salazar M, Phillpot SR, Gleiter H. Acta Mater 2001;49:2713.
[11] Van Swygenhoven H, Spaczer M, Caro A. Nanostruct Mater 1998;10:819.
[12] Van Swygenhoven H, Caro A, Farkas D. Mater Sci Eng A 2001;309–310:440.
[13] Ke M, Hackney SA, Milligan WW, Aifantis EC. Nanostruct Mater 1995;5:689.
[14] Schiotz J, Rasmussen T, Jacobsen KW. Philos Mag A 1996;74:339.
[15] Schiotz J, Di Tolla FD, Jacobsen KW. Nature 1998;391:561.
[16] Shan Z, Stach EA, Wiezorek JMK, Knapp JA, Follstaedt DM, Mao SX. Science 2004;305:654.
[17] Liao XZ, Zhou F, Lavernia EJ, Srinivasan SG, Baskes MI, He DW, et al. Appl Phys Lett 2003;83:632.
[18] Yamakov V, Wolf D, Phillpot SR, Gleiter H. Acta Mater 2002;50:5005.
[19] Chen M, Ma E, Hemker KJ, Wang YM, Cheng X. Science 2003;300:1275.
[20] Rosner H, Markmann J, Weissmuller J. Philos Mag Lett 2004;84:321.
[21] Liao XZ, Zhou F, Lavernia EJ, He DW, Zhu YT. Appl Phys Lett 2003;83:5062.
[22] Van Swygenhoven H, Derlet PM. Phys Rev B 2001;64:224105.
[23] Murayama M, Howe JM, Hidaka H, Takaki S. Science 2002;295:2433.
[24] Kumar KS, Suresh S, Chisholm MF, Horton JA, Wang P. Acta Mater 2003;51:387.
[25] Hasnaoui A, Van Swygenhoven H, Derlet PM. Science 2003;300:1550.
[26] Warner DH, Sansoz F, Molinari JF. Mater Res Soc Symp Proc 2004;791:Q5.31.1.
[27] Lu L, Shen Y, Chen X, Qian L, Lu K. Science 2004;304:422.
[28] Stern EA, Siegel RW, Newville M, Sanders PG, Haskel D. Phys Rev Lett 1995;75:3874.
[29] Van Swygenhoven H, Farkas D, Caro A. Phys Rev B 2000;62:831.
[30] Wolf D. Acta Metall 1989;37:1983.
[31] Wolf D. Acta Metall 1989;37:2823.
[32] Wolf D. Acta Metall Mater 1989;38:781.
[33] Wolf D. Acta Metall Mater 1989;38:791.
[34] Wolf D. J Mater Res 1990;5:1708.
[35] Rittner JD, Seidman DN. Phys Rev B 1996;54:6999.
[36] Randle V. Acta Mater 1997;46:1459.
[37] Singh V, King AH. Scr Mater 1996;34:1723.
[38] Farkas D. J Phys Condens Matter 2000;12:R497.
[39] Dorfman S, Fuks D, Malbouisson LAC, Mundim KC, Ellis DE. Int J Quantum Chem 2002;90:1448.
[40] Dorfman S, Fuks D, Malbouisson LAC, Mundim KC. Comput Mater Sci 2003;27:199.
[41] Chandra N, Dang P. J Mater Sci 1999;34:655.
[42] Namilae S, Chandra N, Nieh TG. Scr Mater 2002;46:49.
[43] Hoagland RG, Kurtz RJ. Philos Mag A 2002;82:1073.
[44] de Koning M, Kurtz RJ, Bulatov VV, Henager CH, Hoagland RG, Cai W, et al. J Nucl Mater 2003;323:281.
[45] Molteni C, Marzari N, Payne MC, Heine V. Phys Rev Lett 1997;79:869.
[46] Suzuki A, Mishin Y. Interf Sci 2003;11:131.
[47] Suzuki A, Mishin Y. Interf Sci 2003;11:425.
[48] Kurtz RJ, Hoagland RG. Scr Mater 1998;39:653.
[49] Kurtz RJ, Hoagland RG, Hirth JP. Philos Mag A 1999;79:665.
[50] Derlet PM, Van Swygenhoven H, Hasnaoui A. Philos Mag 2003;83:3569.
[51] Ballo P, Kioussis N, Lu G. MRS Symp Proc 2001;634:B3.14.1.
[52] Ovid'ko IA, Sheirnerman AG. Acta Mater 2004;52:1201–9.
[53] Frederiksen SL, Jacobsen KW, Schiotz J. Acta Mater 2004;52:5019.
[54] Schiotz J, Vegge T, Di Tolla FD, Jacobsen KW. Phys Rev B 1999;60:11971.
[55] Sansoz F, Molinari JF. Scr Mater 2004;50:1283.
[56] Tadmor EB, Ortiz M, Phillips R. Philos Mag A 1996;73:1529.
[57] Shenoy VB, Miller R, Tadmor EB, Rodney D, Phillips R, Ortiz M. J Mech Phys Solids 1999;47:611.
[58] Miller R, Tadmor E. J Comput Aided Mater Des 2002;9:203.
[59] Foiles SM, Baskes MI, Daw MS. Phys Rev B 1986;33:7983.
[60] Ercolessi F, Adams J. Eur Phys Lett 1993;26:583.
[61] Brokman A, Balluffi RW. Acta Metall 1981;29:1703.
[62] Horstemeyer MF, Baskes MI, Prantil VC, Philliber J, Vonderheide S. Modelling Simul Mater Sci Eng 2003;11:265.
[63] Zhou M. Proc R Soc Lond A 2003;459:2347.
[64] Miller R, Tadmor E, Phillips R, Ortiz M. Modelling Simul Mater Sci Eng 1998;6:607.
[65] Spearot DE, Jacob KI, McDowell DL. Mech Mater 2003;36:825.
[66] Kelchner CL, Plimpton SJ, Hamilton JC. Phys Rev B 1998;58:11085.
[67] The QC method home page. Available from: http://www.qcmethod.com.